Performance and Upgrades for the Electron Cyclotron Heating System on DIII-D

Mirela Cengher, J. Lohr, Y. A. Gorelov, R. Ellis, Egemen Kolemen, D. Ponce, S. Noraky, and C. P. Moeller

***Abstract*— The electron cyclotron heating (ECH) system on the DIII-D fusion reactor consists of six 110-GHz gyrotrons with 6 MW installed power for pulses limited administratively to 5 s in length. The transmission coefficient is better than −1.1 dB for four of the transmission lines, which is close to the theoretical value. A new depressed collector gyrotron was recently installed and is injecting up to 720 kW of power into DIII-D during 2013 tokamak operations. Three of the four dual waveguide launchers, which can steer the RF beams ±20° both poloidally and toroidally, were used for real-time neoclassical tearing mode control and suppression with increased poloidal scanning speed up to 60°/s and positioning accuracy of the beams of ±2 mm at the plasma center. The ECH capabilities on DIII-D are being steadily updated, leading to increased experimental flexibility and high reliability of the system. In the past year, the ECH system reliability reached 87% for 2352 successful individual gyrotron shots into DIII-D. Planning is under way for the addition of two new depressed collector gyrotrons, one at 110 GHz, 1.2 MW and another at 117.5 GHz, 1.5 MW generated power, both of which are in the test stage at Communications and Power Industries.**

***Index Terms*— Antenna, DIII-D, electron cyclotron current drive, electron cyclotron heating (ECH), gyrotron, RF transmission line.**

I. Introduction

THE electron cyclotron heating (ECH) system of the DIII-D fusion reactor [1] has six gyrotrons operating at 110 GHz, and injecting up to 3.5 MW for pulses up to 5 s in length. Each gyrotron is connected to a single mirror matching optics unit (MOU). The MOU mirror directs the RF beam into the waveguide after it has left the gyrotron and produces a Gaussian waist at the waveguide input. The beam then excites the $HE_{1,1}$ mode in the circular waveguide. A carefully designed alignment procedure is used to compensate for the adjustment limitations due to the single mirror design. Power losses in the MOU are around 20% of the total power losses in each system.

Manuscript received July 31, 2013; accepted October 30, 2013. Date of publication April 3, 2014; date of current version July 8, 2014. This work was supported by the U.S. Department of Energy under Grant DE-FC02-04ER54698 and Grant DE-AC02-09CH11466.

M. Cengher, J. Lohr, Y.A. Gorelov, D. Ponce, S. Noraky, and C. P. Moeller are with General Atomics, San Diego, CA 92186 USA (e-mail: cengher@fusion.gat.com; lohn@fusion.gat.com; gorelov@fusion.gat.com; ponce@fusion.gat.com; noraky@fusion.gat.com; moeller@fusion.gat.com).

R. Ellis and E. Kolemen are with the Princeton Plasma Physics Laboratory, Princeton, NJ 08543 USA (e-mail: ellis@fusion.gat.com; ekolemen@pppl.gov).

Color versions of one or more of the figures in this paper are available online at http://ieeexplore.ieee.org.

Digital Object Identifier 10.1109/TPS.2013.2292299

TABLE I
LOSSES IN THE TRANSMISSION LINES

System	Total # Miters 2011	Theoretical transmission waveguide	Measured transmission in the waveguide	Transmission in MOU	Total transmission (w/g and MOU)
System 4	9	83.5% (-0.78 dB)	81.0% (-0.91 dB)	93.3% (-0.30 dB)	75.61% (-1.21 dB)
System 5	9	83.5% (-0.78 dB)	79.4% (-1.00 dB)	95.6% (-0.20 dB)	75.85% (-1.20 dB)
System 6	10	82.3% (-0.84 dB)	81.2% (-0.90 dB)	96.5% (-0.15 dB)	78.37% (-1.06 dB)
System 7	10	82.3% (-0.84 dB)	77.8% (-1.09 dB)	92.5% (-0.34 dB)	71.96% (-1.43 dB)
System 8	10	82.3% (-0.84 dB)	80.1% (-0.96 dB)	94.4% (-0.25 dB)	75.6% (-1.215 dB)
System 10	8	84.8% (-0.72 dB)	81.1% (-0.91 dB)	97.06% (-0.13dB)	78.7% (-1.04 dB)

The 31.75-mm-diameter corrugated waveguide transmission line [2] is evacuated and connects to the tokamak without a window. The transmission efficiency in the six operating waveguide lines is above 77.8% for all operational systems, as shown in Table I. Two alternative methods for testing the beam alignment were developed: a dummy load power measurement, and a calibrated measurement using a four-port RF monitor. Direct beam profile measurements are also used to assess beam quality.

The peak injected energy has been 16.6 MJ for a single tokamak pulse with all six gyrotrons injecting for the full 5 s pulselength.

A new depressed collector gyrotron was installed at the end of 2012 with a new high-voltage (HV) power supply, new transmission line, and new launcher. This system has injected powers of up to 720 kW into DIII-D. The total measured transmission coefficient for this new line was 78.7% and the generated power has been up to 930 kW.

The four dual launchers installed on DIII-D [3] inject the RF power from the tokamak's low-field side. A movable mirror allows the launched RF to be directed over ±20° toroidally to create both co- and counter-current drive, or scanned poloidally over 40° in the tokamak so it can be absorbed at the second-harmonic resonance on nearly all flux surfaces. The elliptical polarization is controlled so that the desired extraordinary or ordinary modes are excited for any injection geometry. Real-time steering of the launcher antennas under control of the DIII-D operating system generates EC driven current, tracking resonant flux surfaces for neoclassical tearing mode (NTM) suppression and control.

Calorimetric monitoring of the gyrotron internal losses is providing additional information for optimal operation and for the output RF power determination [4]. Direct RF power measurements were completed with a high-power long-pulse

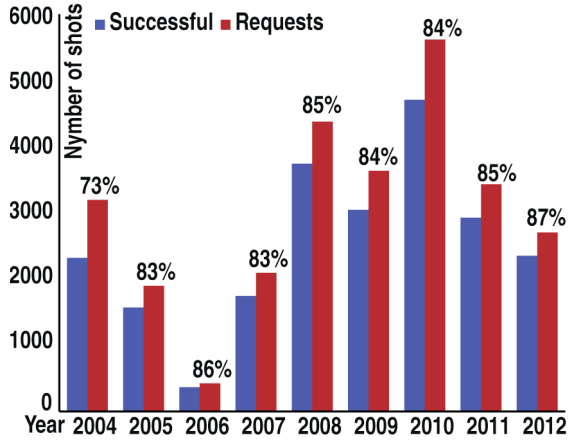

Fig. 1. Succesful shots, individual gyrotron requests, and reliability for the past nine years.

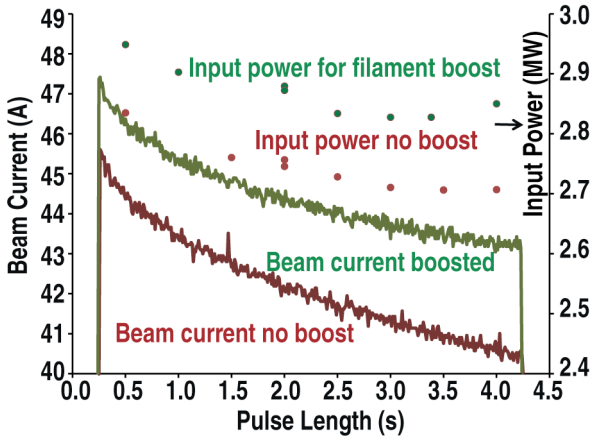

Fig. 2. Gyrotron electron beam current with and without filament boost waveform (with continuous line), and input power (plotted with circles) versus pulselength for the recently installed depressed collector gyrotron. The boost case corresponds to higher input power and higher current (green), and the no-boost (in red) shows lower input power for the lower beam current. For the boost case, the filament voltage is increased by 20%, 6 s before the pulse.

dummy load installed near the tokamak launchers. The dummy load also was placed at the first part of the transmission line; power comparisons were then correlated with gyrotron calorimetry to provide an injected power measurement for each plasma shot accurate to ±5%.

As the capabilities were steadily being upgraded, the system has performed with good reliability. The operational reliability reached 87% for 2012, with 2352 successful shots.

Two systems are undergoing preparation work for the two new gyrotrons that are expected to be installed during 2013, which will bring the total number of gyrotrons in the ECH system to 8.

II. ECH System Overview

A. Installed Gyrotrons

The DIII-D ECH system currently consists of six operational gyrotrons that are installed in the corresponding tanks in the ECH gyrotron vault. The nominal installed power is 6 MW, and the total generated power during operations is 4.5 MW for 5-s pulses. All six gyrotrons were manufactured at Communications and Power Industries (CPI), have a designed pulselength of 10 s, produce Gaussian output beams, and have diamond output windows made with chemical vapor deposition (CVD). To avoid overheating of the collectors during testing and operation, the electron beam is swept over the collector using a sawtooth waveform to reduce the dwell time at the ends of the sweep. The sweep frequency is 5 Hz for five of the gyrotrons and 10 Hz for the depressed collector gyrotron. The overall gyrotron reliability for plasma experiments remained stable at more than 83% in the last nine years, as shown in Fig. 1.

Despite the 1.2-MW designed output power for the 110-GHz depressed collector gyrotron installed in 2013 (gyrotron Chewbacca), the actual generated power is about 25% lower than the design value for long pulses. The typical operational parameters for this gyrotron were $I_{\text{beam}} = 45$ A, $V_{\text{cathode}} = 64.3$ kA, and $V_{\text{body}} = 28.1$ kV. The gyrotron has a 7% drop in beam current during a 5-s pulse, even with maximum allowed filament current boost programs, as shown

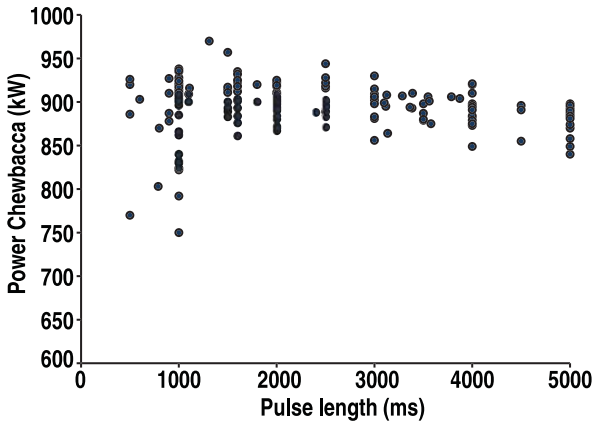

Fig. 3. Generated power measured versus pulselength using a barrel dummy load during testing of the depressed collector gyrotron.

in Fig. 2, where the input gyrotron power, also plotted, shows a corresponding decrease with pulselength due to the drop in current. As a result, the generated power measured during gyrotron testing was lower for longer pulselengths, as in Fig. 3. For very short pulses, the gyrotron did achieve 1.2 MW during factory testing.

The MOUs on the DIII-D ECH system have a single mirror, rather than a pair, to focus and direct the RF beam after it leaves the gyrotron. This limits the ability to translate the beam in the vertical plane. To compensate for this limitation, an offset and tilted spool piece is designed to couple the MOU to the gyrotron. This spool, unique for each gyrotron, places the centroid of the RF beam onto the optical axis of the MOU, allowing a geometrical alignment.

A seventh tank is ready and available for the installation of the next depressed collector gyrotron that is being tested by the producer and is expected to be installed before the end of 2013. The design, construction, and installation of the eighth gyrotron tank, to accommodate the first 117.5 GHz gyrotron, are in progress.

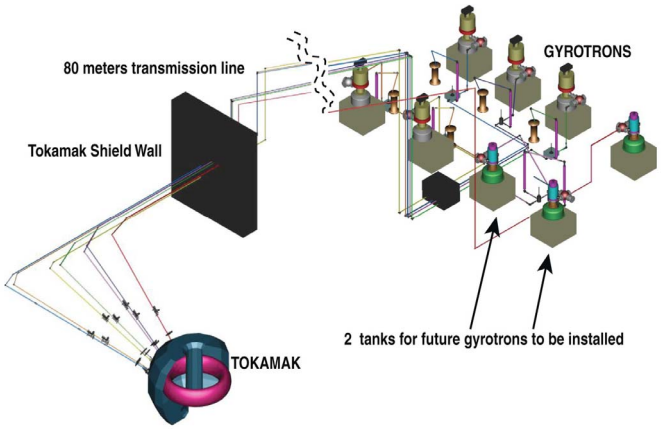

Fig. 4. DIII-D ECH transmission lines layout, showing the six installed gyrotrons and the tanks for the two gyrotrons expected to be intalled in 2013 (not to scale).

B. Transmission Line

The DIII-D waveguide transmission lines (Fig. 4) with average 80 m length, have 8–10 miter bends, including two polarizers for each line, and have an overall efficiency of about 80%, excluding the losses in the MOU. The DIII-D system uses a 31.75-mm-diameter evacuated corrugated waveguide with circular cross section designed for 110 GHz. The lines are all made from aluminum and step-corrugated on the inside with corrugation depth $\sim\lambda/4$ with very low fields at the wall, resulting in low-loss transmission for the $HE_{1,1}$ waveguide mode.

The goal for a good beam alignment to the waveguide is to obtain actual losses that are close to the theoretical transmission line losses [5], [6]. The procedure will be described in Section III-C.

C. ECH Launchers

Four dual launchers are installed for the ECH system on DIII-D. The eight waveguide transmission lines are organized into four groups of two, and each group is routed to the corresponding launcher, mounted on the tokamak vacuum vessel above the equatorial plane.

The four fully articulating dual launchers [3] [Fig. 5(a)] can steer the RF beams poloidally and toroidally $\pm 20°$ in each direction. All were designed and built by the Princeton Plasma Physics Laboratory. Each launcher has a fixed focusing mirror followed by a steering mirror. In the past, two of the six focusing mirrors were damaged during experimental campaigns on DIII-D. The focusing mirrors have not sustained any damage since the installation of a new design with solid Glidcop construction and improved radiation cooling from blackened and sandblasted back surfaces. The steering mirrors are flat and are made from brazed layers of CuCrZr and stainless steel with a CuCrZr overcast on the reflecting surface. These have performed well in service. The temperature at the launcher mirrors is measured during shots with a set of resistance temperature devices (RTDs) mounted at the back of the mirrors. The temperature measurement on the fixed

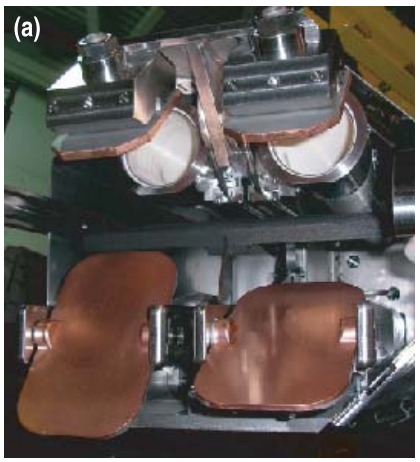

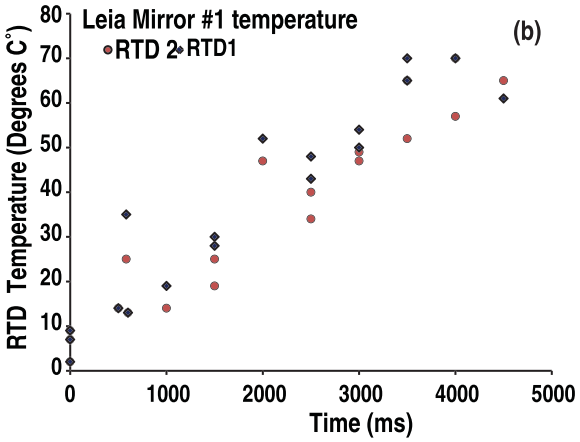

Fig. 5. (a) Photograph of the vacuum side of a DIII-D dual launcher. (b) Back surface temperatures for a fixed mirror. The back surface measurements constrain model calculations, giving the maximum temperatures on the reflecting surfaces.

mirrors showed a modest (<75 °C) increase, as shown versus the pulselength in Fig. 5(b), confirming that the new fixed mirror design is acceptable. Model calculations show a front surface temperature of 300 °C. The mirrors are not actively cooled, but are expected to be able to handle pulses from the future 1.5-MW gyrotrons.

Three of the four dual waveguide launchers were used for real-time NTM control and suppression with poloidal scanning speed up to 60°/s and positioning accuracy of the beams of ± 2 mm at the plasma center under command from the plasma control system (PCS). The RF beam diameter is $\sim$10 cm at the -20-dB contour. The mirror movement in response to a step command is shown in Fig. 6.

An upgrade to new motors is expected to increase the speed by a factor of three, so a sweep over the full 40° of motion will be completed in 200 ms.

D. Control System, Magnets, and Power Supplies

The control system for the DIII-D ECH gyrotrons was designed for flexibility, with functions that are distributed among a number of computers and controllers. A programmable logic controller (PLC) system handles the status and

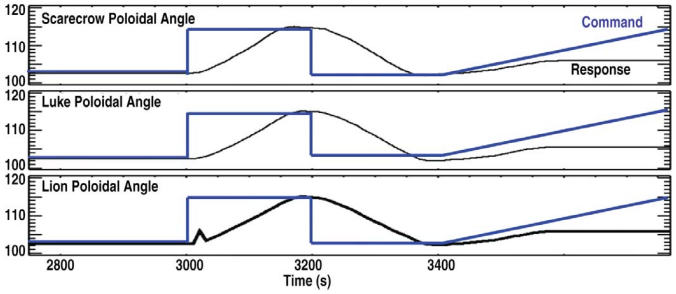

Fig. 6. Response of the poloidal drives for flat steering mirrors on three of the systems.

commands for gate valves, waveguide switches, vacuum, cooling, gyrotron magnets, HV commands and other lower speed interlocks and commands that are compatible with the 20-ms PLC cycle times.

Each gyrotron is assigned a dedicated computer, each magnet is controlled by an individual local PC, and a data server is dedicated for data acquisition. A control server coordinates the operation of the entire system and interfaces to the operators through a LabVIEW user interface. Gyrotrons can be operated in the "group" mode, in which commands apply to any desired subset of the six tubes. This allows timing commands to be sent to all gyrotron control computers simultaneously or to separate the system as desired. The pulse timing is handled by a programmable waveform generator on each system, which can be set up in several modes (continuous and modulated combinations) and different waveforms (square wave, sinusoidal wave, or triangular). The desired waveforms provide the control inputs to the HV power supplies. Waveforms can also be controlled by the DIII-D PCS, either in feedback or preprogrammed mode. Pulse timing can be set locally or from the DIII-D control room.

Fault processing is handled either by a discriminator/trigger module or, for the two newest installations, by a field-programmable gate array (FPGA) system. Eventually, all control and fault processing will be migrated to FPGA format. The FPGA allows greater flexibility in the programming of output power waveform, retry after fault, response to incipient fault, and variable fault response. These features have the potential to increase the operational reliability and flexibility of the system.

The data acquisition system uses both CAMAC and PXI digitizers for archiving the significant waveforms such as RF power, current, voltage, and waveform command, together with the calorimetry data from a number of circuits on the gyrotrons and transmission lines. The calorimetry data is then used to calibrate the RF power pick-up signal. The traces for the microwave power delivered to the tokamak from the individual gyrotrons are calibrated and stored in the DIII-D database after every shot.

The gyrotron magnets in the ECH system are of three basic types but with identical field profiles. The oldest magnet in the system requires both liquid helium (LHe) to cool the coils and liquid nitrogen to cool the cryostat radiation shield. This magnet has been retrofitted with a pulse tube reliquifier, which has a cold finger above the LHe reservoir that reliquifies the boiloff from the reservoir. Another magnet requires regular LHe fills, but has a refrigerator to cool the radiation shield. This magnet has also been recently retrofitted with a reliquifier. The remaining four magnets, supplied with the second group of gyrotrons, are completely cryogen-free and are cooled by compressor refrigerators. No LHe is typically lost from the magnet cryostats.

The electrical power for the gyrotrons is derived from variable ratio transformers with series/parallel strings of solid-state rectifiers that deliver about 110 kVdc to tetrode modulator/regulators located in shielded and access-controlled rooms near the gyrotrons. Two of the gyrotrons have dedicated modulator/regulators and can be controlled independently. The remaining four gyrotrons are powered in two groups of two, with a single tetrode modulator powering two gyrotrons in parallel. Both members of each of these pairs receive the same HV waveform. The power from each gyrotron in these pairs can be routed independently into the tokamak or into the dummy loads. The new depressed collector gyrotron is powered from an HV power supply having a dedicated tetrode modulator and a solid-state crowbar.

The gyrotrons can be modulated by preprogrammed waveforms with different shapes at frequencies up to about 5 kHz or can be controlled by the DIII-D PCS using feedback from a number of diagnostics. Good fidelity is retained up to about 2 kHz.

III. ECH System Performance

A. Power and Reliability

The total power injected into DIII-D has been up to 3.5 MW for 4.5 MW generated. The operational maximum of 5 s for six gyrotrons in the same shot has resulted in a maximum of 16.6 MJ total injected energy in the plasma. The operational maximum is imposed to prolong the collector fatigue lifetime during 5-Hz sweep of the electron beam.

Reliability is calculated for the DIII-D system on a gyrotron-by-gyrotron basis. In the past 8 years, the annual reliability of the ECH system was above 83%, even as new gyrotrons were being added to the system although with some substitution of individual tubes due to failures. The reliability was as high as 87% in the 2012 campaign. The number of successful shots during this campaign was 2352 out of 2703 requested. Over the past nine years, there were 22 771 successful individual shots recorded out of 27 371 total requests.

Injected power calibration is done using the measured gyrotron cavity or internal load power absorption and the measured transmission in each line. Direct power measurements were made calorimetrically, and these were correlated with the calorimetric measurements of power loading on various cooled components of the gyrotron. These measurements were performed at different gyrotron magnet fields and different beam voltages and showed that cavity power loading and the internal load power measurements are linearly correlated with the ECH power at the DIII-D end of the transmission line, as measured in a dummy load installed at the tokamak (Fig. 7). The calibration coefficient was measured with this procedure for each system and was used on a shot-to-shot basis for injected power measurements during experiments.

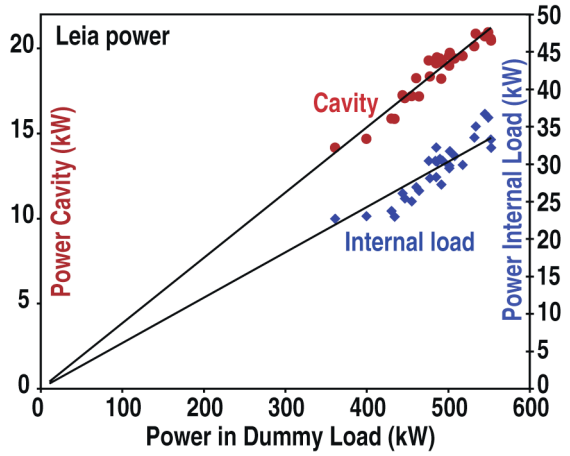

Fig. 7. Gyrotron cavity and internal load power loading versus the power measured in a dummy load at the tokamak.

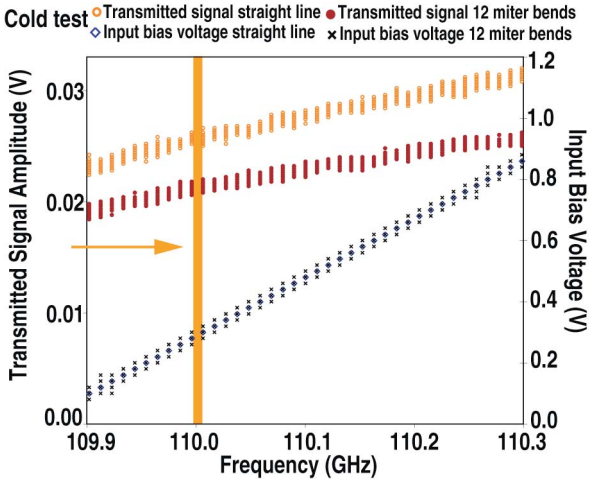

Fig. 8. Cold-test transmission efficiency results showing the transmitted amplitude for a straight waveguide (in orange) and for 12 miter bends (in red), together with the biasing voltage (in blue and black).

The power generated by each gyrotron is slightly detuned from the maximum power that was installed in order to avoid early RF puse termination during DIII-D plasma shots and to increase reliability.

B. Losses in the Transmission Line

Transmission line efficiency is a major issue for high-power microwave systems, so comprehensive sets of measurements were performed to look at the losses in the system.

The power absorbed in the MOU is 3%–7.5% of the generated power, depending on the system. These losses can occur if the beam is not a perfect Gaussian, or if the RF alignment at the waveguide is poor. The theoretical efficiency of excitation of the $HE_{1,1}$ waveguide mode is 98%, so this sets the lower limit on MOU loading. Additional diffraction loss can occur at the MOU mirror because of the finite size of the mirror, and resistive loss is a relatively insignificant 0.1%.

The other main contribution to the total losses comes from the elements of the waveguide transmission line: miter bends, polarizers, and the 80 m of the waveguide. Theoretical calculations of the losses for the 31.75-mm waveguide at 110 GHz [5], [6] are 0.002 dB/m for the circular corrugated waveguide, 0.062 dB for each normal miter bend, and 0.090 dB in polarizing miter bends.

The losses in the miter bends were measured both for low power and high power. The low-power measurement has the advantage that a pure low-loss propagating $HE_{1,1}$ mode can be injected, so the losses due to higher order modes are eliminated, and the results can be compared with the theoretical predictions. The cold-test setup consisted of a Gunn diode biased to scan a frequency range between 109.9 and 110.3 GHz, an $HE_{1,1}$ mode generator, 12 miter bends, and a receiver plus detector on the other end of the line. The measurement was repeated without the miter bends, the replacement being with a similar length of straight waveguide. The results are summarized in Fig. 8. The ratio between the two sets of detector responses was the total transmission coefficient due only to the 12 miter bends. No variation with the frequency was found for this interval, and the measured value for the pure $HE_{1,1}$ transmission coefficient per miter bend was 0.069 ± 0.011 dB, which is consistent with the theoretical prediction. This method ignores some aspects of mode generation and coupling at the miters.

The transmission line efficiencies were measured at high power by moving the same dummy load between the ECH gyrotron vault and the DIII-D machine pit and referencing the calorimetrically measured power in the dummy load to calorimetry on the gyrotron cooling circuits, the internal loads, and cavity, which are proportional to the generated power [7]. As the transmission lines have slightly different lengths, numbers of miter bends, and quality of the propagating mode, the transmission varies from line to line. The measured transmissions, not including the MOU losses, are shown in Table I and range from 77.8% to 81.2%.

The newly installed transmission line for the depressed collector gyrotron has 78.7% transmission, including the MOU losses. This is the best performing line, which is in part due to the excellent quality of the RF beam.

C. RF Beam Alignment

At the input end, the RF power is directed from the MOU into the waveguides, where smaller waveguide is more sensitive to transverse misalignment and the larger waveguide is more sensitive to tilt misalignment.

The beam alignment at the MOU waveguide input, therefore, is a critical step in obtaining a high $HE_{1,1}$ mode content and ultimately high transmission coefficient for each line. An iterative procedure is used for this alignment. The beam angle is measured after the MOU mirror, without waveguide or flange, using the RF beam imaged on thermal paper, or infrared camera images, with the target positioned at several distances from the mirror, as in Fig. 9. The MOU mirror is then adjusted to reduce the angular error and to center the beam, followed by a new measurement and a new adjustment, if necessary. The final alignment angle was less than $0.1° \pm 0.3°$ and the radial offset was less than 0.5 mm for the best case.

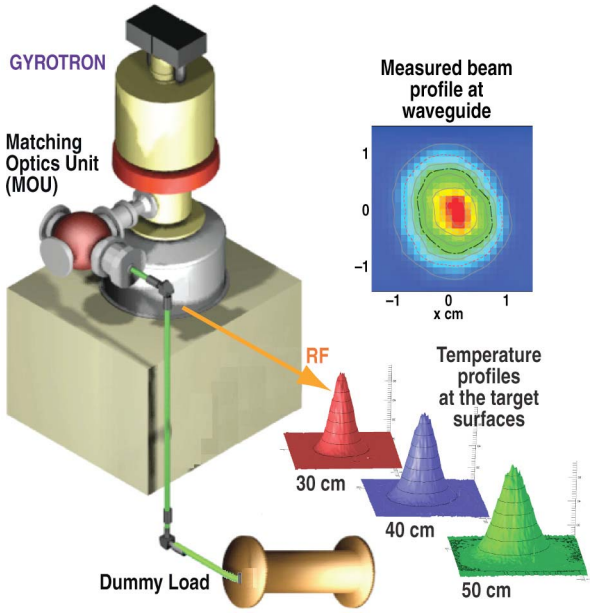

Fig. 9. Experimental setup for the dummy load power measurements and for the beam alignments. For the beam alignment, the MOU flange supporting the waveguide is removed.

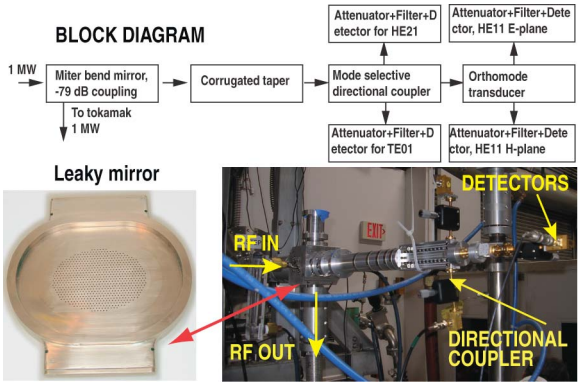

Fig. 10. Experimental setup for the four-port power divider.

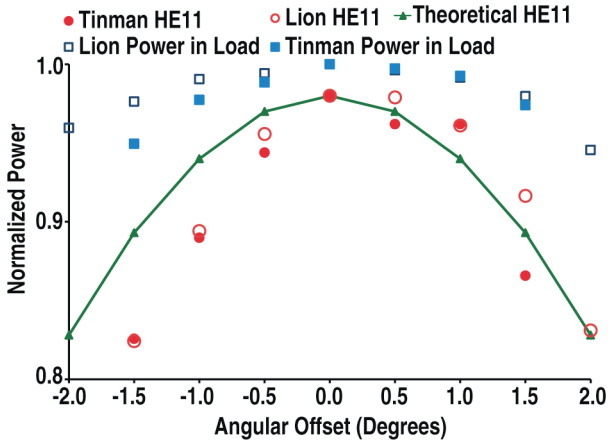

Fig. 11. Departure from best alignment with angular beam offset 0° at the waveguide leading to a decrease in power into the dummy load (red circles) and decrease in $HE_{1,1}$ mode amplitude (blue squares) as shown for two gyrotrons (solid and open points).

D. Tests of Beam Alignment

Because the beam alignment procedures use short RF pulses to avoid breakdown in air, it was necessary to verify that both short and long pulses lead to the same results. The departure from the best beam alignment can be tested using two independent methods: the four-port power divider method, and the dummy load method.

The first method to check the beam alignment uses the measurement of the $HE_{1,1}$ content with a four-port power divider, a leaky mirror, and a mode-selective directional coupler to measure the mode purity directly during the alignment procedure. The divider is a miter bend with a water-cooled mirror featuring an array of through holes that couples −79 dB to one port. A prototype mode analyzer was made in the 31.75-mm waveguide for 1-MW 110-GHz operation and was successfully tested at DIII-D [2]. The low power coupled RF was analyzed for power, mode purity and polarization using a measurement setup (Fig. 10) consisting of an orthomode transducer, a corrugated taper, and mode-selective directional coupler that samples the low-order modes and $HE_{1,1}$. Because the four-port miter is vacuum-compatible at high power, both short and long pulses could be measured. The MOU mirror was rotated up and down to introduce beam misalignment at the waveguide input. The measured $HE_{1,1}$ mode signal versus beam inclination angle was highest for no angular misalignment, 0° angle in Fig. 11, and it dropped as the beam angle was increased to introduce misalignment. The measurements were performed for two of the gyrotrons, and the results are shown in red circles. The theoretical $HE_{1,1}$ mode content versus beam angle is also plotted in Fig. 11 (with green triangles) and shows the same trend as the measured $HE_{1,1}$ mode content. These tests confirmed that the best alignment corresponds to the maximum $HE_{1,1}$ signal and minimum $HE_{2,1}$ and $TE_{0,1}$ signals. A new version of the power divider was built and it is in the initial testing phase.

The second alignment test was based on a calorimetric power measurement in a dummy load with two miter bends between the MOU waveguide input and the load, as in the setup shown in Fig. 9. As the MOU mirror was rotated up and down to introduce beam misalignment at the waveguide input, the power for 1-s pulses was measured in the dummy load versus the beam angle, which is plotted (with blue squares) in Fig. 11. As expected, the amount of power lost in the miter bends increases with misalignment, so the power transmitted to the dummy load decreases as the beam departs from the optimum alignment.

IV. Conclusion

DIII-D has a flexible and capable ECH system, with high installed power, and is continuously being upgraded. Over the past 8 years, good reliability was maintained, even as new gyrotrons were added in the system, bringing the total installed power to 6 MW. Power and transmission in the system are carefully measured, and total injected power is calibrated on a shot-to-shot basis. Transmission line performance is consistent with theoretical predictions for the individual components on

the DIII-D ECH system thanks to the alignment methods that have been developed. Transmission was measured and is greater than 75% for five of the six transmission lines.

A new 110-GHz depressed collector gyrotron was installed and is now operated with power injected into the tokamak up to 720 kW and 930 kW generated. This gyrotron operates with a new HV power supply, a new dual launcher, and newly installed waveguide transmission line.

Two new gyrotrons are expected to be installed in 2013–2014. The first is a 110-GHz depressed collector gyrotron that is being tested by the manufacturer, and is identical in design to the one installed on DIII-D. The second new gyrotron has been designed to generate 1.5 MW. It is a depressed collector diode design with CuCrZr collector, and will be the first tube at DIII-D to operate at the higher frequency of 117.5 GHz, to maximize the plasma performance and decrease trapping at the highest possible magnetic field. The 117.5-GHz gyrotron is scheduled for delivery by CPI to DIII-D at the end of 2013. The upgrades to the DIII-D ECH system will bring the installed power to 8 MW, and increase the injected RF power to 5.5 MW.

Planning has begun for a further significant upgrade leading to generated power up to 10 MW and an increase of the RF frequency for all gyrotrons to 117.5 GHz. The long-term plan for ECH on DIIID calls for 10 gyrotrons, each of which will generate 1.5 MW, for pulselengths appropriate for the capability of the tokamak, approximately 10 s. This will result in injected RF power of 12 MW from 10 gyrotrons.

REFERENCES

[1] J. Lohr, M. Cengher, J. L. Doane, Y. A. Gorelov, C. P. Moeller, D. Ponce, *et al.*, "The multiple gyrotron system on the DIII-D tokamak," *J. Infr. Millim. Terahertz Waves*, vol. 32, no. 3, pp. 253–273, 2010.

[2] M. Cengher, J. Lohr, D. Ponce, Y. A. Gorelov, C. P. Moeller, and M. Shapiro, "Transmission lines power measurements for the 110 GHz electron cyclotron heating system on DIII-D and gyrotron operational performance," in *Proc. 35th Int. Conf. Infr. Millim. Terahertz Waves*, Sep. 2010, pp. 1–2.

[3] R. Ellis, J. Hosea, J. Wilson, R. Prater, and R. Callis, "Design of the dual high power, long pulse steerable ECH launcher for DIII-D," in *Proc. 14th Topical Conf. Radio Freq. Power Plasma, Amer. Inst. Phys. Conf.*, vol. 595. pp. 318–322, 2011.

[4] M. Cengher, *et al.*, "Measurements of the ECH power and of the transmission line losses on DIII-D," in *Proc. 15th Joint Workshop Electron Cyclotron Emission Electron Cyclotron Reson. Heating*, 2008, pp. 483–489.

[5] J. L. Doane, "Propagation and mode coupling in corrugated and smooth-wall circular waveguides," *Infr. Millim. Waves*, vol. 13, no. 1, pp. 123–170, 1985.

[6] J. L. Doane and C. P. Moeller, "HE_{11} mitre bends and gaps in a circular corrugated waveguide," *Int. J. Electron.*, vol. 77, no. 4, pp. 489–509, 1994.

[7] M. Cengher, J. Lohr, I. A. Gorelov, W. H. Grosnickle, D. Ponce, and P. Johnson "Calorimetric measurements of the radio-frequency power and of the transmission line losses on the DIII-D ECH system," *Fusion Sci. Technol.*, vol. 55, no. 2, pp. 213–218, 2009.

[8] R. A. Olstad, R. W. Callis, M. Cengher, J. L. Doane, Y. A. Gorelov, H. J. Grunloh, *et al.*, "Progress on corrugated waveguide components suitable for ITER ECH&CD transmission lines," in *Proc. 17th Joint Workshop Electron Cyclotron Emission Electron Cyclotron Reson. Heating*, 2012, pp. 04020-1–04020-6.

Authors' photographs and biographies not available at the time of publication.